

Plasma Sci. Technol. **24** (2022) 054004 (10pp) https://doi.org/10.1088/2058-6272/ac41c1

Effects of O_2 addition on the plasma uniformity and reactivity of Ar DBD excited by ns pulsed and AC power supplies

Feng LIU (刘峰), **Yue ZHUANG** (庄越), **Yulei ZHAO** (赵昱雷), **Jie CHEN** (陈洁) **and Zhi FANG** (方志)

College of Electrical Engineering and Control Science, Nanjing Tech University, Nanjing 211816, People's Republic of China

E-mail: fangzhi@njtech.edu.cn

Received 8 September 2021, revised 8 December 2021
Accepted for publication 9 December 2021
Published 9 May 2022

Abstract

Dielectric barrier discharges (DBDs) have been widely used in ozone synthesis, materials surface treatment, and plasma medicine for their advantages of uniform discharge and high plasma-chemical reactivity. To improve the reactivity of DBDs, in this work, the O_2 is added into Ar nanosecond (ns) pulsed and AC DBDs. The uniformity and discharge characteristics of Ar ns pulsed and AC DBDs with different O_2 contents are investigated with optical and electrical diagnosis methods. The DBD uniformity is quantitatively analyzed by gray value standard deviation method. The electrical parameters are extracted from voltage and current waveforms separation to characterize the discharge processes and calculate electron density n_e. The optical emission spectroscopy is measured to show the plasma reactivity and calculate the trend of electron temperature T_e with the ratio of two emission lines. It is found that the ns pulsed DBD has a much better uniformity than AC DBD for the fast rising and falling time. With the addition of O_2, the uniformity of ns pulsed DBD gets worse for the space electric field distortion by O_2^-, which promotes the filamentary formation. While, in AC DBD, the added O_2 can reduce the intensity of filaments, which enhances the discharge uniformity. The ns pulsed DBD has a much higher instantaneous power and energy efficiency than AC DBD. The ratio of Ar emission intensities indicates that the T_e drops quickly with the addition of O_2 both ns pulsed and AC DBDs and the ns pulsed DBD has an obvious higher T_e and n_e than AC DBD. The results are helpful for the realization of the reactive and uniform low temperature plasma sources.

Keywords: nanosecond pulse power supply, dielectric barrier discharge, discharge uniformity, oxygen addition

(Some figures may appear in colour only in the online journal)

1. Introduction

Dielectric barrier discharge (DBD) can produce large area low temperature plasma at a large variety of conditions (gas pressure, electrode structure, and power supply parameter) [1–3], which makes it widely used in air pollution control [4, 5], material surface treatment [6–8], plasma biomedicine [9] and energy conversion. One of the advantages of DBD is that the dielectric layer between the electrodes can prevent the increase of the discharge current into arc and keep the discharge under uniformity in atmospheric pressure [3, 10]. But at atmospheric pressure, especially with the addition of admixture to improve plasma-chemical reactivity, the uniformity of DBDs is still not satisfied for many applications because usually there are a lot of short-live conductive micro-discharge filaments existing in DBDs [11]. With most of the energy and active species restricted into the filaments, there are low energy efficiency, uneven treatment, and local over-heating problems in the DBDs in the filamentary discharge mode.

Traditionally, DBDs are excited by AC power supplies, and recently, with the development of pulse power technology, the application of nanosecond (ns) pulse power supply in the excitation in DBDs becomes one of important methods to improve the discharge uniformity. It is because the short discharge duration can further limit the formation of filaments and prevent the streamer-to-spark transition. Besides the improvement of the discharge uniformity, the energy efficiency of the pulsed DBDs can be improved compared with AC DBDs because more energy goes into energetic electrons production other than gas heating [12–15]. The high reduced electric field E/n caused by the high voltage slew rate and the high density chemical species produced by energetic electrons would enhance the plasma-chemical efficiency. Therefore, the investigations of the discharge characteristics and applications of the pulsed DBDs attract much attention to improve discharge uniformity, energy efficient, plasma activity, and treatment effects [16]. Walsh *et al* compared the efficiency of pulse and high frequency excited Ar DBDs and concluded that the electron density and atomic oxygen content in pulsed plasma were 3.9 and 3.3 times higher than those excited by high frequency, respectively [17]. Jiang and Yang *et al* respectively studied and compared the optical images of AC and pulsed DBDs under different conditions [18, 19]. Wang *et al* investigated the discharge characteristics of AC and ns pulsed coaxial DBDs and found that the outside wall temperature of the AC coaxial DBD reached 158 °C and was much higher than that of the ns pulsed DBD at 64.3 °C after 900 s operation [20]. Zhang *et al* studied the regime transitions between streamer discharge, diffuse discharge, and surface discharge in ns pulsed DBD using high resolution temporal–spatial spectra and instantaneous exposure images [21]. Yu *et al* studied the ns pulsed DBD temporally resolved evolution by ICCD images [22].

Meanwhile, the amounts and kinds of the active species in plasmas are also critical important in many applications because those species participate physicochemical processes [23]. Usually, to improve the uniformity of atmospheric DBDs, the discharges need operate in inert gases, such as Ar and He, and there is lack of active and functional radicals for plasma-chemical processing. One of the solutions is the addition of additives (such as O_2, H_2O, CF_4) to produce reactive species (such as O, OH, H, NO, HO_2, O_3, F) [24–26]. Among of those additives, O_2 plays a crucial role because it can produce oxidative radicals, such as O and O_3, which are important in thin film deposition and etching, VOCs oxidation, and biomedical treatment applications. Fang *et al* used Ar DBD for PET film surface hydrophilic modification and found that appropriate amount of oxygen addition (0.3%) can enhance the treatment effect [27]. Weng *et al* inactivated bacteria with radio-frequency Ar DBD and found the optimum of inactivation of *E. coli* treatment effect at the addition of 0.5% oxygen and 30 s exposure time [28]. Hicks *et al* studied the process optimization of $Ar/O_2/CF_4$ plasma treatment of diamond substrate smoothing and the effect of removing subsurface polishing damage [29].

However, the added oxygen would affect the plasma properties more complicated. A proper amount of oxygen admixture could increase the discharge by Penning effect with metastable molecules of inert gases. However, with excessive oxygen addition, it will reduce the electron density by forming O_2^- and quench the metastable molecules, which exacerbate the distortion of the electric field distribution and the non-uniformity of discharge. For the purpose of realizing uniform and reactive oxygen containing DBD plasma sources, the understanding of the discharge phenomena is very important, which reveals the effect of O_2 in the plasma processing.

Considering the widely use of AC and pulsed power supplies in the excitation of DBDs, in this work, the effects of oxygen addition on the characteristics of ns pulsed DBD and AC DBD are compared and quantitative analyzed. The measured voltage and current waveforms are separated to reveal the ignition and extinction of the discharge processes, and to estimate n_e. The tendency of T_e under different O_2 contents is derived from the two emission lines by optical emission spectroscopy (OES) measurement.

2. Experimental setup

Figure 1 shows the experimental setup, which includes a discharge reactor, electrical and optical measurement systems, gas supply system, and AC and ns pulse power supplies. The stainless steel reactor can be vacuumed with a rotary pump. A pair of 50 mm diameter parallel plates is used as electrodes, and an 80 mm diameter 2 mm thick quartz glass is used as dielectric barrier. The gas gap between electrode plates is fixed at 2 mm. The voltage range of the AC power supply is 0–30 kV and frequency is from 1 Hz to 15 kHz. The ns pulse power supply can provide 0–15 kV peak pulse high voltage and 1 Hz to 100 kHz pulse repetition frequency. The rising and falling times, pulse width of the pulse voltage are in the ranges of 50 ns to 500 ns, and 0–5000 ns, respectively. In the experiment, the frequencies of both the power supplies are fixed at 10 kHz, and the rising and falling times are fixed at 50 ns, which can produce discharges on the rising and falling edges. The pulse width of the pulse voltage is fixed at 800 ns for a better discharge uniformity and stability.

The electrical measurement system is composed of a digital oscilloscope (Tektronix 3054), a high voltage probe (North Star PVM-5) and a current coil (Pearson Electronics Inc. 2877) for the voltage–current measurement from the power supplies, and a differential probe (LDP-6002) for the voltage measurement on a 2.2 nF measuring capacitor (C_r) for electrical parameters calculation. A Canon EOS 6D camera is used to record the discharge image with 1/6 s exposure time. The OES is measured by an Ocean Optic HR4000CG spectrometer (0.7 nm resolution). The purity Ar and O_2 are used as discharge gases and a bottle of mixture gas of Ar/O_2 with 1% O_2 is used when the O_2 content is below 1% for the purpose of precise ratio control.

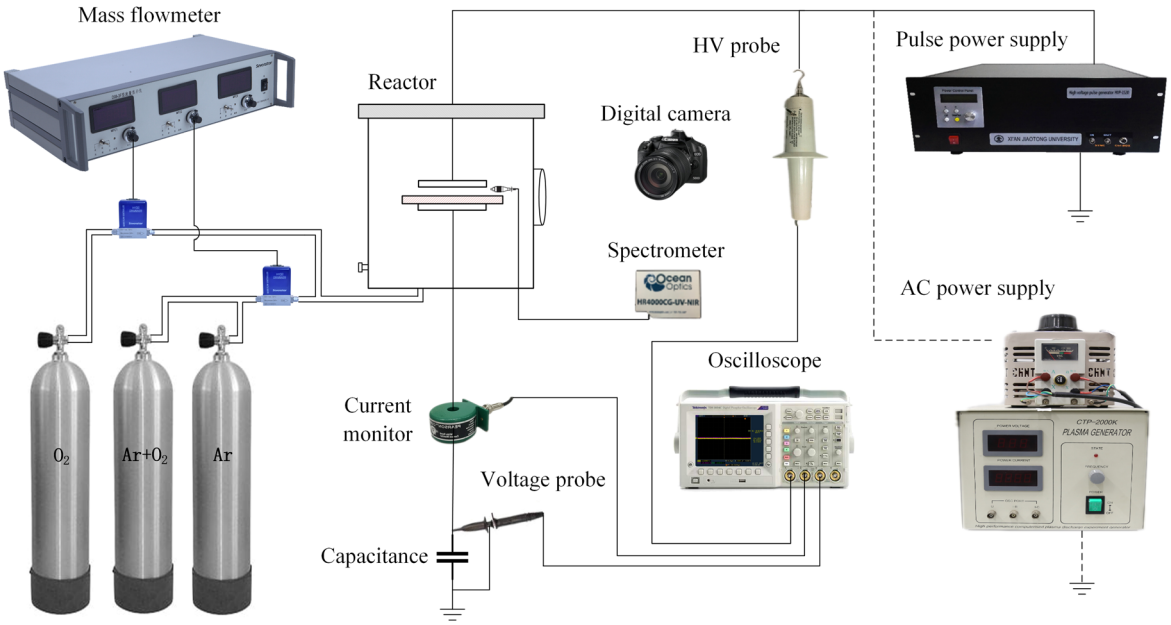

Figure 1. The schematic of the DBD experimental setup.

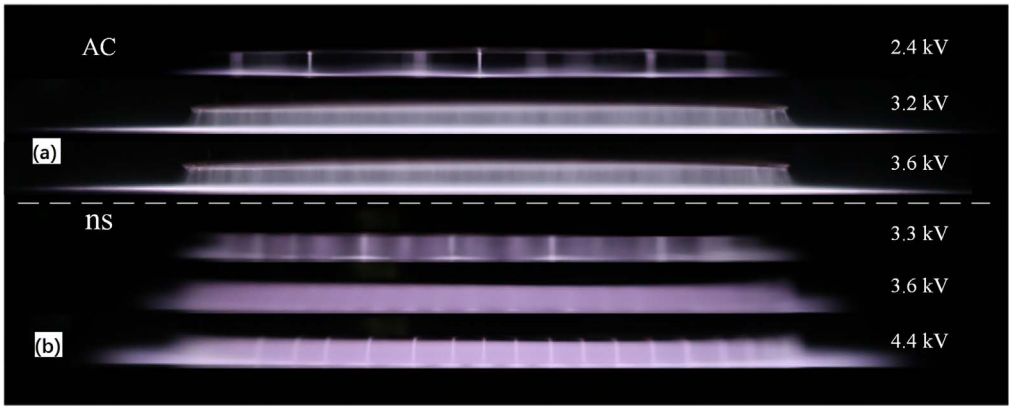

Figure 2. The discharge images of DBD excited by AC (a) and ns pulse (b) power supplies.

3. Results and discussion

3.1. Discharge uniformity of argon DBD

Figure 2 shows the optical images of the AC and ns pulsed Ar DBDs, respectively. It can be seen that the AC DBDs are in filamentary mode with the applied voltage from 2.4 to 3.6 kV. At a lower voltage, 2.4 kV, the discharge cannot be full of the space between the electrodes and just with isolated filaments. With 3.2–3.6 kV applied voltage, the discharge occupies all of space but is still in filamentary mode. Similarly, the Ar DBD excited by the ns pulsed power supply shows isolated filaments in the discharge space at a lower voltage, 3.3 kV. With the increasing of the applied voltage, the plasma fills in the whole discharge space without obvious filaments at 3.6 kV. The Ar DBD excited by ns pulsed power supply is more uniform, which is due to the short rise time of pulse voltage, thus terminating the transition from Townsend glow discharge to serious filamentous phase. However, as the applied voltage further increases to 4.4 kV, filaments appear in the discharge due to high voltage.

The experimental results show that the applied voltage range of ns pulse Ar DBD is larger than that of AC, which is due to the over-voltage breakdown of pulse discharge, and the gas needs higher voltage to be ionized. From figure 2, when the voltage of AC is 2.4 kV, several clear and countable weak filaments are generated locally in the discharge space. With the increase of the applied voltage to 3.6 kV, the electric field intensity increases, the collision ionization increases, and the electron avalanche intensifies, resulting in the discharge filament filling the whole space, the discharge intensity increases, and the discharge is still uneven. When the applied voltage of ns pulse is 3.3 kV, the discharge does not fill the whole space as AC DBD when the voltage is 2.4 kV. While, except the filaments, more diffuse plasma fills the gap in ns pulsed DBD than AC DBD. With the applied voltage increasing, the filament gradually fills the whole space and fuses in the ns pulsed

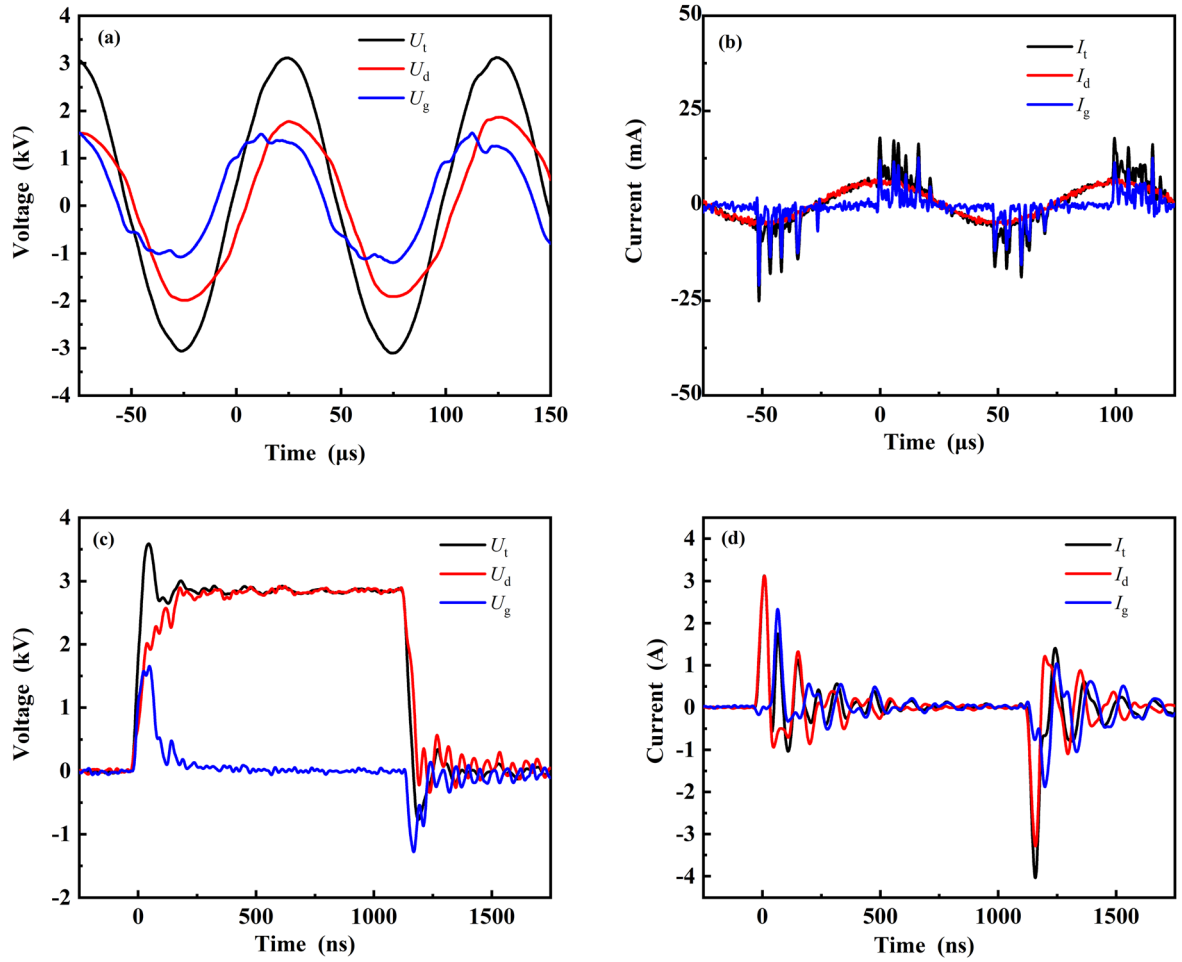

Figure 3. The discharge gap voltage separation waveforms of AC DBD (a) and ns pulsed DBD (c), and the current separation waveforms of AC DBD (b) and ns pulsed DBD (d).

DBD. When the applied voltage reaches 3.6 kV, it is hard to observe the filament in the ns pulsed DBD, and the discharge is with good uniformity. With 4.4 kV applied voltage of ns pulsed DBD, a few bright streamers are generated in the space, and the discharge uniformity of ns pulsed DBD decreases.

Although the discharge images can be qualitatively judged by eye, it is impossible to quantitatively get the value of the discharge uniformity. To quantitatively analyze the discharge uniformity, some researchers have developed different image processing methods based on fast Fourier transform, spatial correlation function, and gray level histogram [30–32]. In our previous research, we have developed a method of gray value standard deviation (GVSD) to quantitatively analyze the discharge uniformity from the optical images [33]. The pixel gray values of discharge area can be obtained with graying processing, and the gray values x_n of the middle horizontal line of the discharge area are averaged to get the averaged gray value x_m. Then, the normalized value $\overline{x_n}$ can be obtained:

$$\overline{x_n} = \frac{x_n - x_m}{v}, \tag{1}$$

where v is the variance of pixel value. Then, the gradient value of $\overline{x_n}$ can be obtained with differentiation processing, which is the value of GVSD and can be used to indicate the uniformity of discharge.

With the above GVSD method for discharge uniformity, the GVSD values of the AC DBD images at 2.4, 3.2, and 3.6 kV are 8.25, 4.34, and 4.68, and the GVSD values of the ns pulsed DBD images at 3.3, 3.6, and 4.4 kV are 5.48, 0.73, and 3.45. The lower GVSD value indicates the better discharge uniformity. The values of GVSD and the discharge images are consistent. For the GVSD below 1, the discharge seems very uniform and it can be defined as a uniform discharge, as shown in the ns pulsed DBD at 3.6 kV.

3.2. Electrical characteristics of argon DBD

Because the DBD uniformity is strongly associated with the electrical characteristics of discharge, the electrical parameters of the ns pulsed DBD and AC DBD are calculated. For DBD structure, the applied voltage U_t is dropped on the gas gap and the dielectric barrier, as U_g and U_d, and the measured current I_t with current probe measurement is the sum of the displacement current, I_d, and conduct current, I_g. As the

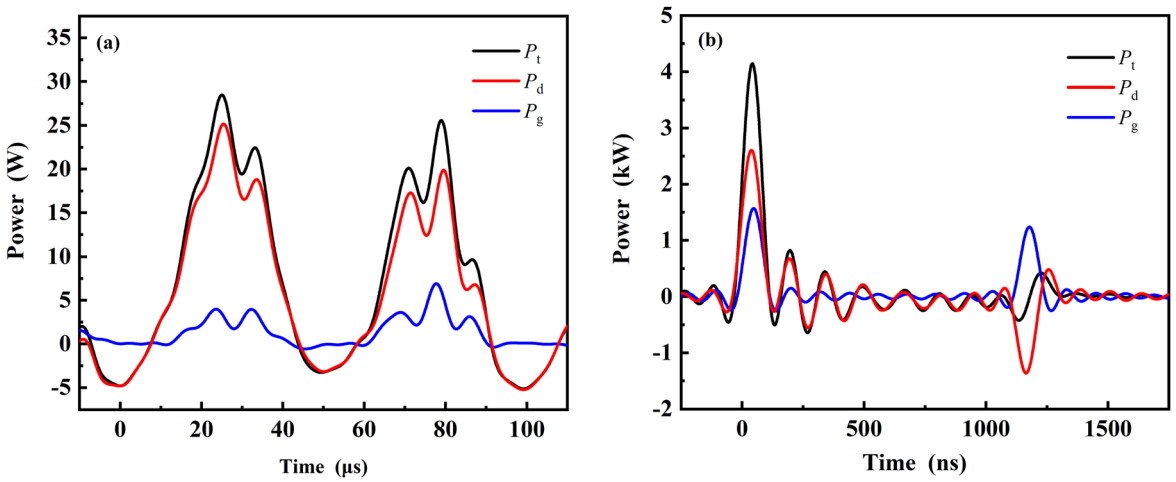

Figure 4. The power separation waveforms of DBD excited by AC (a) and ns pulse (b).

method described in our previous studies [10, 33, 34], U_d can be estimated with an insert capacitor in the ground side and U_g is obtained with the subtraction of U_d from U_t. I_d can be obtained without discharge under same applied voltage by pumping the reactor to vacuum or replace the inert gas with air. I_g can be obtained with the subtraction of I_d from I_t. The separations of the applied voltage of AC and ns pulsed DBDs are shown in figures 3(a) and (c), and the separations of the measured currents are shown in figures 3(b) and (d).

From the above figures that the peak values of U_g of AC and ns pulsed DBDs are much smaller than those of the applied voltages for part of the voltages dropped on the dielectric barriers. The peak value of U_g of AC DBD is about 1.2 kV and the peak value of U_g of ns pulsed DBD is about 1.6 kV. In ns pulsed DBD, the duration time of the U_g of the rising side of the pulse is very small, about 100 ns, which prevents the electron avalanches over development. At the falling side of the pulse, the accumulated charge causes the reverse stroke. In AC DBD, the duration time of the U_g is very long, about 25 μs, which results in many current pulses in a very long time scale. The electron avalanches are under lasting electric field and the filaments are easily formed. The peak value of I_g separated from ns pulsed DBD is about 2.4 A, which is much higher than that at mA level under AC DBD. The amount of transferred charge (Q) has an important influence on the reaction rate, efficiency and application effect of plasma. In general, the Q can be calculated by integrating I_g over a period. However, due to the bipolar nature of I_g during AC and ns pulse DBD discharge, the Q at the rising edge and the falling edge will offset each other. Therefore, the method of calculating Q in the whole discharge process is to add the absolute value of Q in the first half cycle and the second half cycle, as shown in formula (2):

$$Q = \int_0^{\frac{T}{2}} i_g(t)\mathrm{d}t + \left| \int_{\frac{T}{2}}^{T} i_g(t)\mathrm{d}t \right|. \tag{2}$$

According to the above formula, the values of Q of AC and ns pulsed DBDs are 142.5 nC and 151.1 nC, respectively. The results show that there are more active particles produced in ns pulsed DBD than in AC DBD.

Discharge power is an important parameter to describe the intensity of discharge, including the instantaneous total power P_t, instantaneous gas gap power P_g and instantaneous dielectric layer power P_d, which can be obtained by equations (3)–(5):

$$P_t = U_t \times I_t, \tag{3}$$

$$P_g = U_g \times I_g, \tag{4}$$

$$P_d = P_t - P_g. \tag{5}$$

The P_t, P_g and P_d of Ar DBDs excited by AC and ns pulse are shown in figure 4. From figure 4 that the peak value of P_t under AC DBD is around 30 W, and that of ns pulsed DBD is about 4.2 kW. The P_g of DBD excited by ns pulse is also larger than the value of AC DBD. Using the instantaneous power data, the corresponding average total power $\overline{P_t}$, average air gap power $\overline{P_g}$, average dielectric layer power $\overline{P_d}$ and energy efficiency η can be calculated by equations (6)–(9):

$$\bar{P}_t = \frac{1}{T}\int_0^T P_t\mathrm{d}t, \tag{6}$$

$$\bar{P}_g = \frac{1}{T}\int_0^T P_g\mathrm{d}t, \tag{7}$$

$$\bar{P}_d = \bar{P}_t - \bar{P}_g, \tag{8}$$

$$\eta = \frac{\bar{P}_g}{\bar{P}_t} \times 100\%. \tag{9}$$

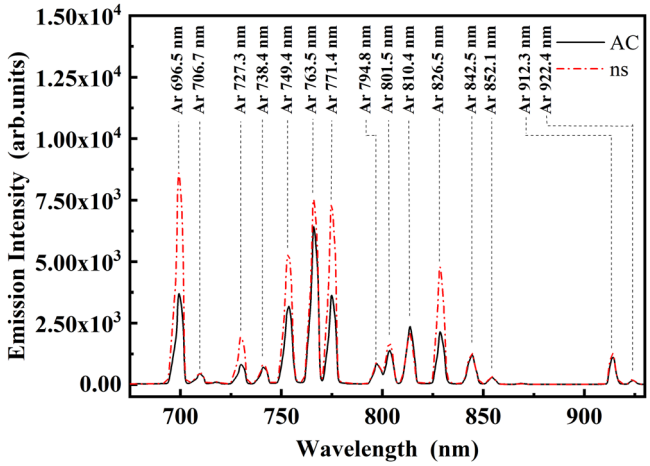

Figure 5. The optical emission spectra of AC and ns pulse excited Ar DBD.

Under the experimental conditions, $\overline{P_t}$ is 8.6 W, $\overline{P_g}$ is 1.5 W, $\overline{P_d}$ is 7.1 W and η is 17.4% of DBD under AC excitation, and $\overline{P_t}$ is 2.9 W, $\overline{P_g}$ is 1.9 W, $\overline{P_d}$ is 1 W and η is 65.5% of DBD under ns pulse excitation. Compared the above results, it can be seen that the $\overline{P_t}$ of AC DBD is larger than of ns pulsed DBD, but the η of AC DBD is lower than that of ns pulsed DBD, which indicates that a lot of energy was consumed by dielectric layer capacitive load in DBD during AC excitation.

3.3. Optical emission spectra of argon DBD

In DBD, a large number of electrons and ions are produced when the applied voltage exceeds the breakdown voltage and with the electric field in space, the electrons are accelerated and gain energy to become high-energy electrons, which eventually lead to the excitation, ionization, and dissociation of the background molecules into active species. Some excited species can be observed by the optical emission spectra. In Ar DBD, most of the active species are excited states of argon atoms and the excited states of argon atoms transit back to the lower level excited or ground states to release photon, which can be observed

$$e + Ar \rightarrow e + Ar^*. \quad (10)$$

The intensities of the observed optical emission spectra represent the relative number densities of the excited species. Figure 5 shows the emission spectra of AC Ar DBD and ns pulsed Ar DBD. The applied voltage of AC power supply is fixed at 3.2 kV, and that of ns pulse power supply is fixed at 3.6 kV. From figure 5, it can be seen that the excited species of Ar DBD excited by AC and ns pulse discharge are the same. But the intensities of the emission lines are different. The optical emission intensities of excited Ar in ns pulsed DBD are higher than those in AC DBD. Taking the Ar line (696.5 nm) as an example, under the same conditions, the optical emission intensity in ns pulsed DBD is about 2.31 times that in AC DBD. By comparing the emission intensities of the excited Ar, it can be concluded that ns pulsed Ar DBD can produce plasma with more active particle and higher reactivity than AC DBD. The main reason is that the applied voltage of ns pulse power supply can rise to a value much higher than the breakdown voltage of gas in a short time, so it can provide a larger initial electric field strength, generate a greater instantaneous power, and significantly improve the reaction rate, so as to produce more active particles in the discharge space.

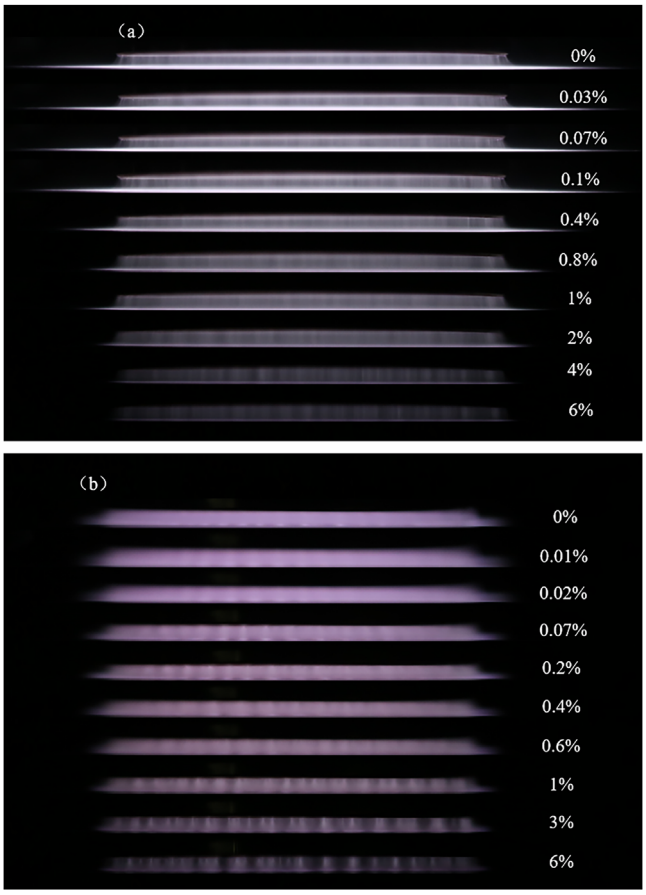

Figure 6. The discharge images of DBD excited by AC (a) and ns pulse (b) power supplies at various oxygen additions.

3.4. Discharge uniformity with different oxygen contents

With the addition of oxygen, it participates in the discharge process and affects the discharge uniformity and reactivity. Figure 6 shows the discharge images of Ar DBDs under AC and ns pulse excitations with different oxygen contents. The applied voltage of AC power supply is fixed at 3.2 kV, and that of ns pulse power supply is fixed at 3.6 kV. To quantitatively analyze the variation of Ar DBD uniformity with oxygen content under different power supply conditions, the GVSD of the discharge images of DBDs excited by different power supplies at various oxygen additions are calculated. Figure 7 is the GVSD value of figure 6. The quantitative analysis of the optical discharge images shows that the regularity of uniformity change reflected by the GVSD value is consistent with the luminescent images.

It can be seen that under high frequency AC excitation, when the oxygen content is in the range of 0%–0.2%, the discharge is more intense and the discharge gap is full of

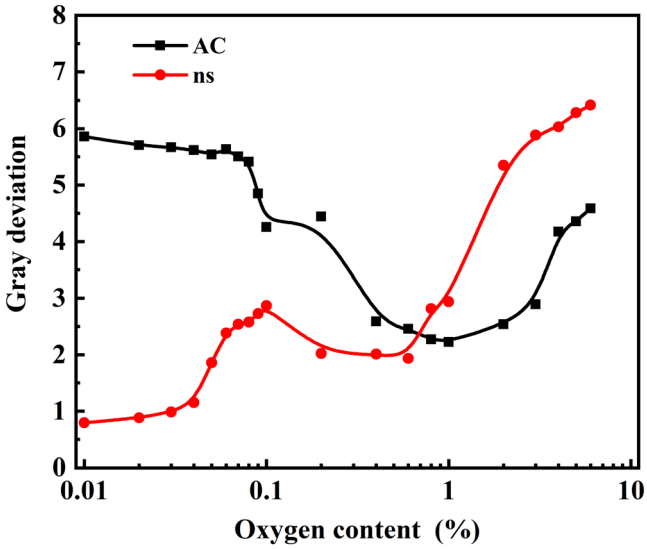

Figure 7. The gray value standard deviation of DBD excited by AC and ns pulse power supplies at various oxygen additions.

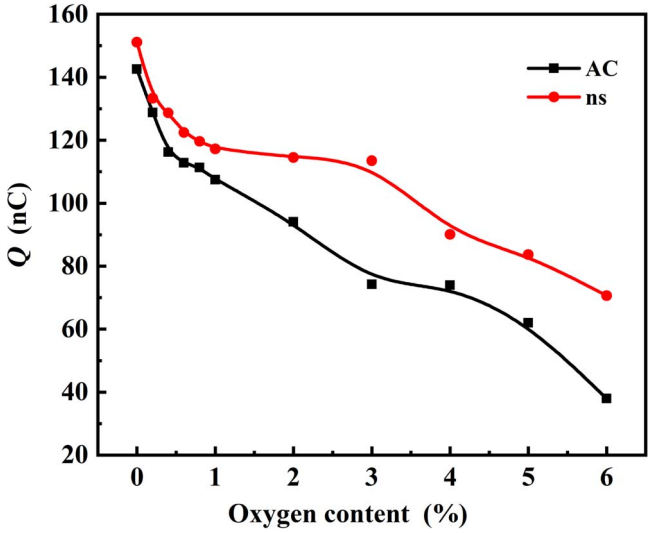

Figure 8. The variations of transported charges of DBD excited by AC and the ns pulse power supplies at various oxygen additions.

bright filaments, and the uniformity is poor. With the increase of oxygen content, the electronegative gas O_2 will adsorb a large number of electrons and inhibit the development of electron avalanche, resulting in the decrease of discharge intensity, the decrease of bright discharge filaments. When the oxygen content increases to 1%, the discharge is relatively stable, the discharge filaments become dense, and the uniformity is improved. In this stage, the GVSD decreased from 5.34 to 2.22. After that, with the increase of oxygen content to 6%, due to serious space electric field distortion, the discharge intensity further weakens, the number of discharge filaments decreases, the uniformity decreases again, and the GVSD gradually increased to 4.58. When the ns pulse is used as the excitation power supply, under the condition of extremely low oxygen content (0%–0.03%), the discharge uniformity under different oxygen content has little change and the GVSD of the discharge image is less than 1. This is due to the Penning ionization between Ar metastable particles and O_2, which produces a large number of electrons and leads to the cross fusion of electron avalanches, so that the uniformity of discharge can be maintained. With the increase of oxygen content, the uniformity of DBD discharge decreases gradually. When the oxygen content reaches 0.1%, bright filaments appear in the discharge gap, the discharge begins to be unstable, and the uniformity decreases rapidly. In this stage, the GVSD increased to 2.86. With the increase of oxygen content to 0.2%–0.6%, the discharge filaments become dark, the number of filaments increases, the distribution of filaments in the discharge space tends to be uniform, and the GVSD value is maintained at about 2. When the oxygen content increases to 6%, a large number of metastable particles of Ar were quenched and the number of space free electrons was further weakened. Therefore, the discharge intensity becomes weaker, the brightness of filament discharge decreases, and the GVSD value decreases. When O_2 was added further (0.6%–6%), O_2 adsorbed a large number of electrons to form O_2^- ions, which led to the electric field in space further distortion and the poor uniformity. The excess O_2 cannot fill the whole discharge space. In this stage, the GVSD further increased to 4.58.

3.5. Electrical properties with different oxygen contents

Figure 8 shows the variation trend of the transfer charge with oxygen addition in DBD under AC and ns pulse excitations. Because O_2 is a kind of electronegative gas, it can adsorb electrons, inhibit the development of electron avalanche, and lead to the decrease of discharge filaments. It can be seen that with the increase of oxygen addition, the transfer charge (Q) presents a continuous downward trend. When the oxygen content increases from 0% to 6%, the Q decreases from 142.5 nC to 37.9 nC of DBD under AC excitation, and from 151.1 to 70.6 nC of DBD under ns pulse excitation. Under the same oxygen content, the value of Q of DBD excited by ns pulse is larger than that excited by AC. The reason is that the DBD discharge time of ns pulse excitation is much shorter than that of DBD AC excitation in a single cycle, and ns pulsed DBD has higher U_g and I_g. Figure 9(a) shows the variation trend of average discharge power of DBD excited by AC and ns pulse with oxygen addition. As shown in figure 9, with the increase of O_2 content, $\overline{P_t}$, $\overline{P_g}$ and $\overline{P_d}$ of AC and ns pulsed DBDs decreased. Among them, when the oxygen content increases from 0% to 6%, the $\overline{P_t}$ of AC decreases from 8.6 to 6.8 W, and $\overline{P_g}$ of AC DBD decreases from 1.5 to 0.7 W. The $\overline{P_t}$ of ns pulsed DBD decreases from 2.9 to 0.9 W, and $\overline{P_g}$ of ns pulsed DBD decreases from 1.9 to 0.5 W.

Figure 9(b) shows the curves of energy efficiency with oxygen addition of DBDs under the excitation of two kinds of power sources. It can be found from figure 9(b) that the η of DBDs of AC and ns pulse excitation decreases with the addition of O_2. Among them, η of ns pulsed DBD is in the range of 56.68%–67.01%, which is much larger than that of DBD of AC excitation (11.03%–17.17%). Generally, the energy efficiency is mainly related to the charge utilization rate and dielectric heat loss. Due to the short time interval

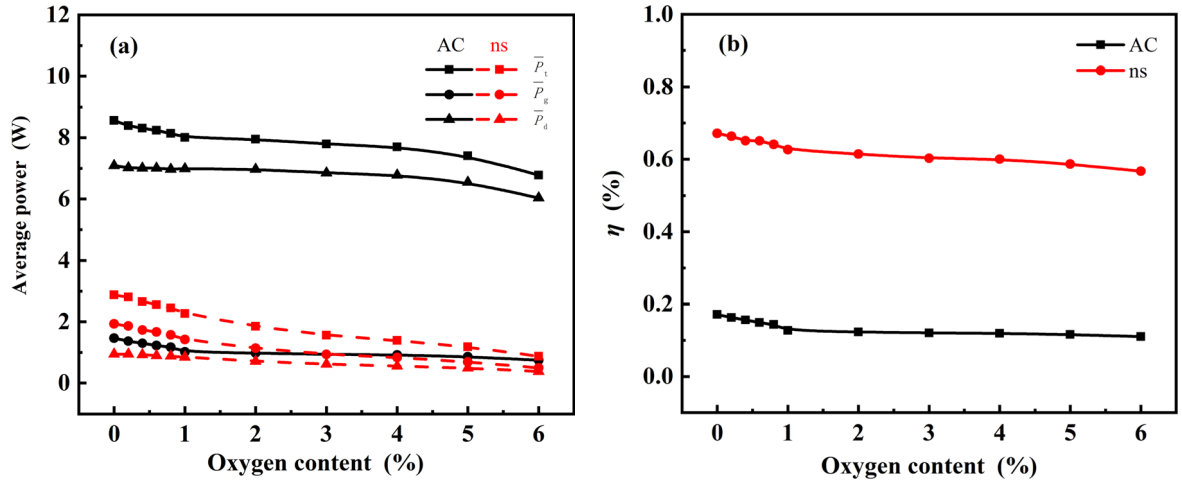

Figure 9. The variations of averaged power (a) and energy efficiency (b) of DBD excited by AC and ns pulse power supplies at various oxygen additions.

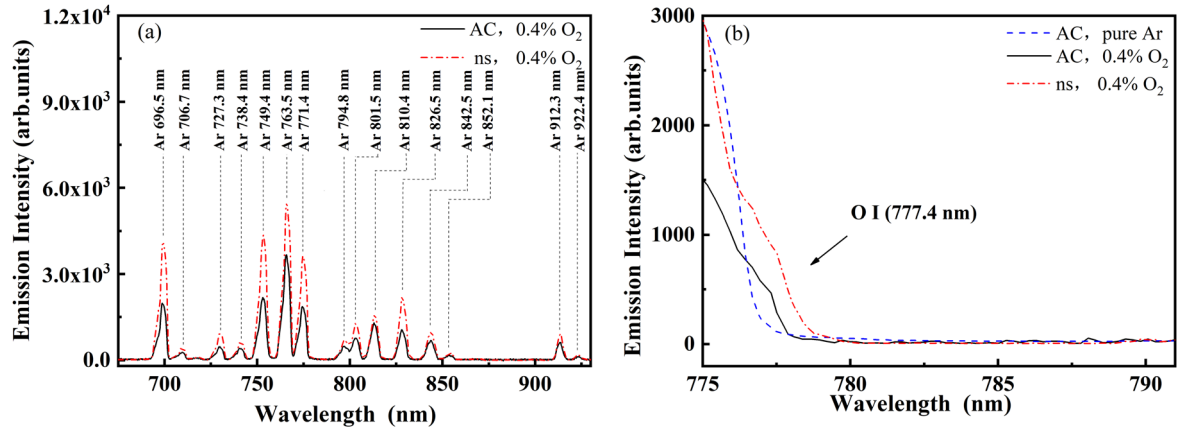

Figure 10. The optical emission spectra of (a) AC and ns pulse excited Ar DBD at 0.4% O_2, and (b) the enlarged spectra of AC Ar DBD, AC and ns pulse excited Ar DBD at 0.4% O_2.

between the two discharges of ns pulse, the charge will not dissipate immediately after the discharge at the rising edge of the voltage, but will still be on the surface of the dielectric barrier or in the gap, which is conducive to the generation of discharge at the falling edge of the pulse voltage. Therefore, the charge utilization rate of ns pulse DBD is higher. Because the duration of ns pulse voltage is very short, the degree of energy concentration on the surface of dielectric is reduced, so the energy loss is less. On the other hand, because O_2 is a kind of electronegative gas with high electron affinity, the higher the oxygen content is, the more electrons it adsorbs and the faster the quenching speed of active particles is. Therefore, the energy efficiency decreases continuously with the increase of oxygen content.

3.6. Optical emission spectra with different oxygen contents

Figure 10 shows the emission spectra of DBD excited by AC and ns pulse with oxygen content of 0.4%. After adding oxygen into Ar, the composition of the main spectral lines observed from Ar/O_2 DBD excited by two kinds of power sources has no obvious change. However, a small amount of O I (777.4 nm) can be found (as shown in the enlarged part in figure 10 with the spectra of AC DBD in pure Ar as a reference), and the intensity of O line of AC DBD is smaller than that of ns pulsed DBD. The reason is that the energy for the production of the upper state of O I (777.4 nm), O ($3p^5P$), is higher than the energy of the observed Ar emission lines at 4p states (around 13 eV). The energies for the ground state O atom production and O ($3p^5P$) excitation from ground state O are 5.1 eV and 3.6 eV [35], according to reactions (11) and (12), and 10.7 eV, respectively. Then, the O ($3p^5P$) is mainly produced by the direct electron impact dissociation excitation, which needs 15.8 eV or 14.3 eV, and ns pulsed DBD has a higher electron temperature than the AC DBD. Therefore, the O I (777.4 nm) intensity is much weaker than the Ar emissions and the intensity of O line of ns pulsed DBD is larger than that of AC DBD. The energy of metastable Ar is 11.72 eV [10], which can dissociate O_2 molecular but cannot ionize the O_2 molecular (12.06 eV ionization energy [36]). But the upper states of Ar lines at 4p states with around 13 eV can collide and ionize O_2 molecular to produce more

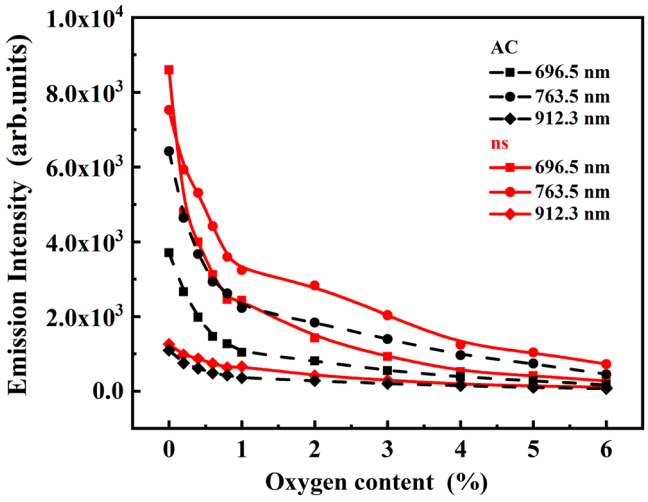

Figure 11. The optical emission intensities of the Ar lines of DBDs excited by AC and ns pulse power supplies at various oxygen contents.

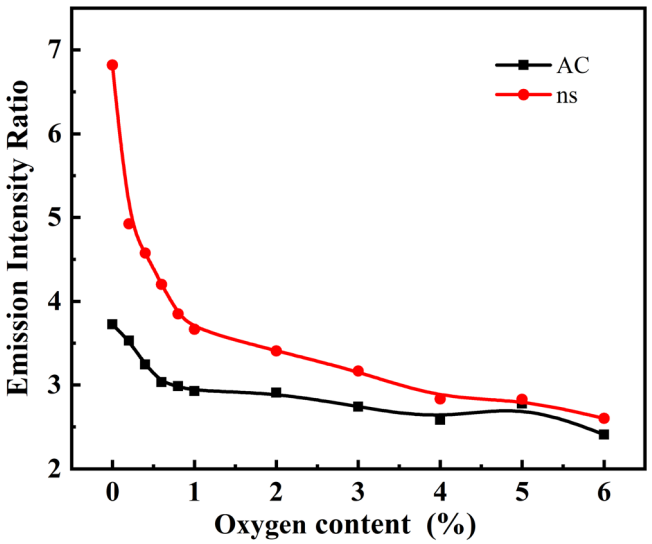

Figure 12. The ratio of the emission intensities of Ar I (696.5 nm) and Ar I (912.3 nm) in AC and ns pulsed DBDs at various oxygen contents.

electrons

$$e + O_2 \rightarrow e + O + O, \tag{11}$$

$$e + O_2 \rightarrow O + O^-, \tag{12}$$

$$Ar(4p) + O_2 \rightarrow Ar + O_2^+ + e. \tag{13}$$

Figure 11 shows the variation trend of the peak intensity of typical particles with oxygen concentration of DBDs under the excitations of two kinds of power sources. The typical optical line intensities under AC and ns pulsed DBDs decreased with the oxygen content increasing, and the typical line intensities of AC DBD are smaller than those of ns pulsed DBD. Taking the Ar I (696.5 nm) as an example, the intensity of the line decreased by 95.3% under AC excitation and 96.8% under ns pulse excitation after 6% oxygen added. This shows that a large number of electrons are adsorbed by O_2 to form O_2^- ions, which reduces the electron number density in space. As a result, the discharge intensity is weakened and the optical emission intensity of Ar line decreases significantly.

The emission intensity I of Ar excited by electron collision can be given by formula (14) [10, 33]:

$$I \propto C_\lambda A \tau [\mathrm{Ar}] n_e \int_\varepsilon^\infty \sigma_i^x(\varepsilon) f(\varepsilon) \sqrt{\varepsilon}\, \mathrm{d}\varepsilon, \tag{14}$$

$$I \propto C_\lambda A \tau [\mathrm{Ar}] n_e k, \tag{15}$$

where C_λ, A and τ are the spectral response of the optical measurement system, Einstein coefficient, and effective lifetime, respectively. $\sigma_i^x(\varepsilon)$ is the excitation cross-section and $f(\varepsilon)$ is the electron energy distribution function (EEDF). Considering the EEDF can be seen as Maxwell's function for the electron local equilibrium, EEDF determines the value of T_e. $\int_\varepsilon^\infty \sigma_i^x(\varepsilon) f(\varepsilon) \sqrt{\varepsilon}\, \mathrm{d}\varepsilon$ is proportional to the excitation rate k and equation (14) can be present as equation (15). [Ar] is the ground state Ar density.

The change of experimental conditions results in the changes of the electron number density n_e and electron temperature T_e. The ratio of two Ar emission intensities at different wavelengths λ with different excitation energies can eliminate the effect of n_e and is only determined by the ratio of k, as shown in equation (16). The ratio of k reflects the electron energy distribution of energetic electrons for the two excitation processes and the equation (16) can be rewritten as equation (17). With the ratio of k and the Bolzmann solver BOLSIG + code [37], the electron excitation energy T_e can be obtained [10]:

$$\frac{I_1}{I_2} = \frac{C_{\lambda 1} A_1 \tau_1 \lambda_1^{-1} k_1}{C_{\lambda 2} A_2 \tau_2 \lambda_2^{-1} k_2}, \tag{16}$$

$$\frac{k_1}{k_2} = \frac{C_{\lambda 2} A_2 \tau_2 \lambda_2^{-1} I_1}{C_{\lambda 1} A_1 \tau_1 \lambda_1^{-1} I_2}. \tag{17}$$

From equation (17), it can be seen that for the determination of T_e, the spectral response of different emission lines should be measured and the effective lifetime of the upper states should be obtained. The effective lifetime τ can be expressed by equation (18).

$$\frac{1}{\tau} = \frac{1}{\tau_0} + \sum_q k_q^x [Q], \tag{18}$$

where τ_0 is the radiative lifetime, $[Q]$ is the quencher q number density, and k_q^x is the collisional quenching rate coefficient. Considering the small amount of O_2 addition and the uncertainty of collisional quenching rate coefficient, the accurate value of the ratio of k is hard to be obtained, which results in the uncertainty of the value of T_e. However, it is still possible to get the tendency of T_e with variable parameters for the purpose of comparation [33].

Because the Ar I (696.5 nm, excitation energy: 13.3 eV) and the Ar I (912.3 nm, excitation energy: 12.9 eV) lines are separated from other lines, and the excitation energy difference is about 0.4 eV. Therefore, it can use the ratio of Ar I (696.5 nm) and Ar I (912.3 nm) intensities to express the relative concentration of high excited state particles and low excited state particles, which reflects the trend of T_e with different O_2 contents. Figure 12 shows the ratio of Ar I (696.5 nm) and Ar I (912.3 nm) emission intensities of DBDs under AC and ns pulse

excitations at different O_2 contents. With the increase of O_2 content, the ratios of Ar I (696.5 nm) to Ar I (912.3 nm) spectral intensities of DBDs under the excitations of the two kinds of power supplies decease continually and the ratio of spectral intensities of AC DBD is lower than that of ns pulsed DBD. It means ns pulsed DBD has a higher T_e than AC DBD, and it is more obvious under low oxygen content. Assuming DBD in uniform status, the electron density, n_e, can also be calculated with the drift velocity of electron, discharge area, and the peak values of U_g as described in our former study [33]. The result shows that n_e is $2.26 \times 10^{17}\,m^{-3}$ for ns pulsed Ar DBD and $1.15 \times 10^{17}\,m^{-3}$ for AC Ar DBD and with 6% oxygen content, n_e drops to $1.52 \times 10^{17}\,m^{-3}$ for ns pulsed Ar DBD and $3.67 \times 10^{16}\,m^{-3}$ for AC Ar DBD.

4. Conclusion

In this work, the uniformity and reactivity of AC and ns pulsed Ar/O_2 DBD are studied with optical and electrical measurements. With GVSD analysis, the discharge uniformity is obtained quantitatively and it is shown that the ns pulsed DBD has a much better uniformity than AC DBD. Compared with the AC DBD, the ns pulse DBD has higher peak value of U_g, I_g, Q, and total instantaneous powers. The maximum energy efficiency of ns pulse excitation is 65.5%, while that of AC excitation is only 17.4%. With the 0.03% O_2 addition, the GVSD of the ns pulsed DBD still keeps below 1, which indicates the uniform discharge. With more O_2 addition, the uniformity of ns pulsed DBD gets worse for the space electric field distortion by O_2^-, which promotes the filamentary formation. For AC DBD, the intensity of filaments is weakened by the attachment effect of the added O_2, which enhances the discharge uniformity. The T_e is indicated by the ratio of two Ar emission intensities. The result shows that the ns pulsed DBD has an obvious higher T_e than AC DBD. With the addition of O_2, the T_e of both ns pulsed and AC DBDs drops quickly. With the O_2 addition from 0% to 6%, the n_e of ns pulsed Ar DBD decreases from $2.26 \times 10^{17}\,m^{-3}$ to $1.52 \times 10^{17}\,m^{-3}$, and the n_e of AC Ar DBD decreases from $1.15 \times 10^{17}\,m^{-3}$ to $3.67 \times 10^{16}\,m^{-3}$.

Acknowledgments

This work is supported by National Natural Science Foundation of China (Nos. 52037004 and 51777091).

References

[1] Brandenburg R 2017 *Plasma Sources Sci. Technol.* **26** 053001
[2] Kogelschatz U 2003 *Plasma Chem. Plasma Process* **23** 1
[3] Bruggeman P J, Iza F and Brandenburg R 2017 *Plasma Sources Sci. Technol.* **26** 123002
[4] Wang T *et al* 2012 *Plasma Chem. Plasma Process* **32** 1189
[5] Zhang Q P *et al* 2016 *Sci. Rep.* **6** 27572
[6] Shao T *et al* 2010 *Appl. Surf. Sci.* **256** 3888
[7] Yuan H *et al* 2018 *Surf. Coat. Technol.* **344** 614
[8] Vallade J *et al* 2014 *J. Phys. D: Appl. Phys.* **47** 224006
[9] Fridman G *et al* 2008 *Plasma Process. Polym.* **5** 503
[10] Liu F, Huang G and Ganguly B 2010 *Plasma Sources Sci. Technol.* **19** 045017
[11] Zhang Y H *et al* 2019 *Plasma Sci. Technol.* **21** 074003
[12] Williamson J M *et al* 2006 *J. Phys. D: Appl. Phys.* **39** 4400
[13] Shao T *et al* 2012 *Europhys. Lett.* **97** 55005
[14] Kettlitz M *et al* 2013 *Plasma Sources Sci. Technol.* **22** 025003
[15] Zhang C *et al* 2014 *Phys. Plasmas* **21** 103505
[16] Shao T *et al* 2018 *High Volt.* **3** 14
[17] Iza F, Walsh J L and Kong M G 2009 *IEEE Trans. Plasma Sci.* **37** 1289
[18] Jiang H *et al* 2011 *IEEE Trans. Plasma Sci.* **39** 2076
[19] Yang D Z *et al* 2013 *Appl. Phys. Lett.* **102** 194102
[20] Wang Q *et al* 2018 *Plasma Sci. Technol.* **20** 035404
[21] Zhang L *et al* 2019 *Nanomaterials* **9** 1381
[22] Yu S *et al* 2016 *Phys. Plasmas* **23** 023510
[23] Liu F *et al* 2021 *Plasma Sci. Technol.* **23** 064002
[24] Du Y J *et al* 2017 *J. Phys. D: Appl. Phys.* **50** 145201
[25] Liu Y *et al* 2018 *J. Phys. D: Appl. Phys.* **51** 114002
[26] Bai C J *et al* 2018 *J. Phys. D: Appl. Phys.* **51** 255201
[27] Fang Z *et al* 2017 *IEEE Trans. Plasma Sci.* **45** 310
[28] Weng C C *et al* 2009 *Int. J. Radiat. Biol.* **85** 362
[29] Hicks M L *et al* 2019 *J. Appl. Phys.* **125** 244502
[30] Ye Q Z *et al* 2003 *IEEE Trans. Plasma Sci.* **41** 540
[31] Rong M Z *et al* 2010 *IEEE Trans. Plasma Sci.* **38** 966
[32] Zhang Y *et al* 2016 *Vacuum* **123** 49
[33] Liu F *et al* 2021 *J. Appl. Phys.* **129** 033302
[34] Miao C R *et al* 2018 *Eur. Phys. J.* D **72** 57
[35] Ono R and Oda T 2009 *Plasma Sources Sci. Technol.* **18** 035006
[36] Babaeva N Y *et al* 2005 *J. Vac. Sci. Technol.* A **23** 699
[37] Hagelaar G J M and Pitchford L C 2005 *Plasma Sources Sci. Technol.* **14** 722